Supplementary Materials for

Detected Climatic Change in Global Distribution of Tropical Cyclones

H. Murakami, T. L. Delworth, W. F. Cooke, M. Zhao, B. Xiang, and P.-C. Hsu

Correspondence to: hir.murakami@gmail.com and pangchi.hsu@gmail.com

This PDF file includes:

Figs. S1 to S6
Table S1
References (*1*–*6*)

www.pnas.org/cgi/doi/10.1073/pnas.1922500117

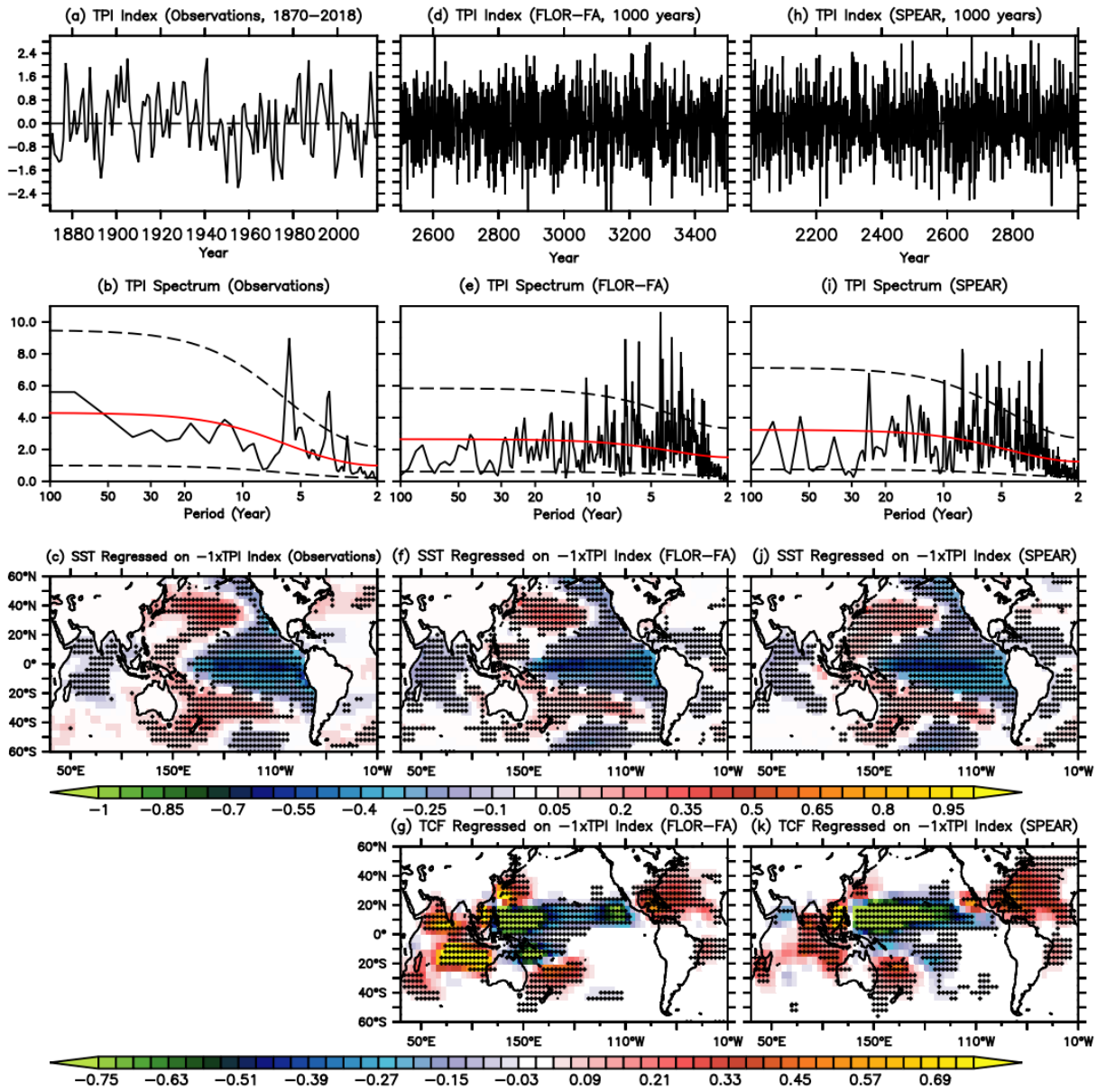

Fig. S1. Observed and simulated IPO index and regression of SST and TCF.

To evaluate the internal variability in the tropical Pacific, especially for Interdecadal Pacific Oscillation (IPO), the observed and simulated Triple Index for the IPO index (TPI, *1*) was examined. The TPI is based on the difference between the SST anomalies averaged over the central equatorial Pacific (R1: 10°S–10°N, 170°E–90°W) and the averages of the SSTAs in the Northwest (R2: 25°N–45°N, 140°E–145°W) and Southwest Pacific (R3: 50°S–15°S, 150°E–160°W). TPI comprises the three SST anomalies [R1 – (R2+R3)/2.0]. The periods for the climatology are 1971 to 2000 for observations and all the simulation years for the model control simulations, respectively. Panel (a) shows time series of TPI using observations (1870–2018; HadISST, *2*). Panel (b) shows the power spectrum of TPI. Panel (c) denotes the regressed SST anomaly on the TPI index with flipped sign to represent the impact of negative IPO phase on SST [units: K σ^{-1}]. (d–f) As in (a–c), but for the piControl of FLOR-FA. (h–j) As in (a–c), but for the piControl of SPEAR. (g, k) As in (f, j), but for the regression of simulated TCF on the

simulated TPI index with flipped sign [units: number σ^{-1}]. The red lines in (b, e, i) represent the Markov "Red Noise" spectrum; black dashed lines represent the lower (5%) and upper (95%) Markov confidence bounds. Dotted marks in (c, f, j, g, k) indicate the correlation coefficients between the TPI index and SST are statistically significant at the 95% significant level according to a *t*-test. The last 1,000 years of the piControl experiments were analysed.

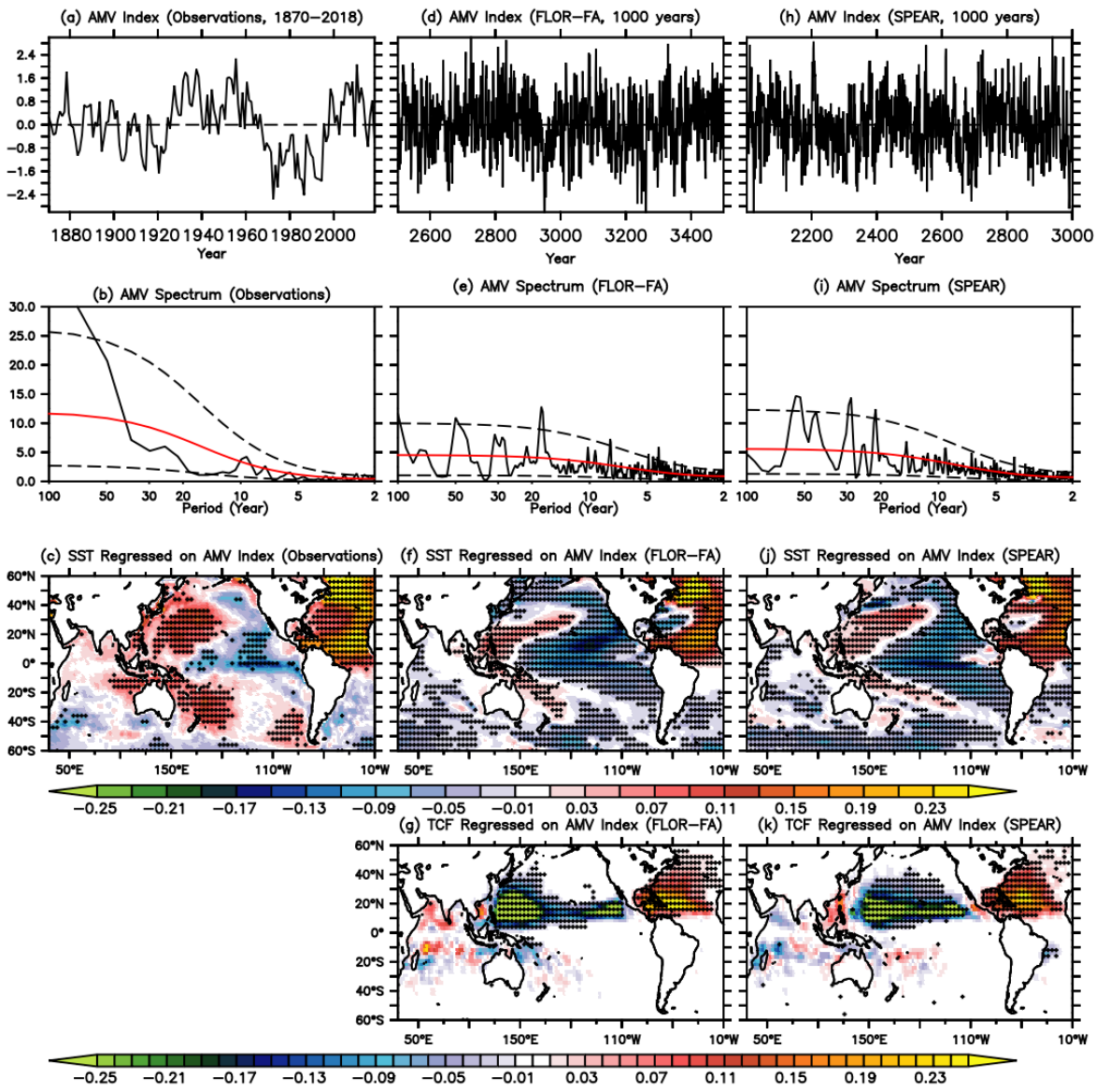

Fig. S2. As in Fig. S1, but for AMV.

The AMV index is defined as the area-average SST anomaly over the North Atlantic (0–70°N, 90°W–0) minus the global mean SST anomaly.

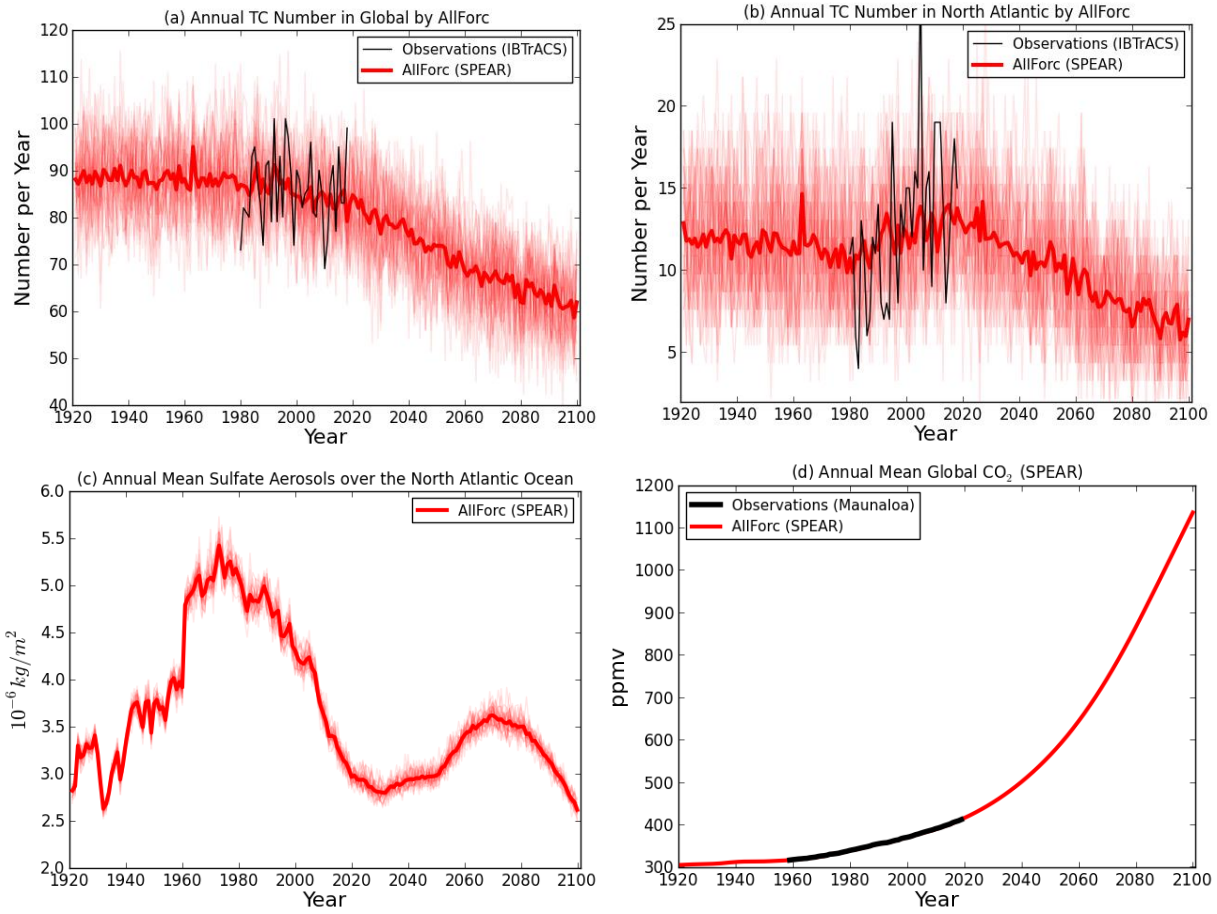

Fig. S3. Time series of TC numbers, sulfate aerosols, and CO_2 concentration from the AllForc experiments by SPEAR.

To reveal long-term evolution of simulated and projected TC numbers associated with anthropogenic aerosol and greenhouse gases, results of the AllFoc experiments by SPEAR from 1921 to 2100 are shown. (a) annual global TC number [units: number per year]; (b) annual TC number in the North Atlantic [units: number per year]; (c) annual mean sulfate aerosols over the North Atlantic Ocean [5°N–45°N, 10°W–90°W; units: 10^{-6} kg m^2]; and (d) annual global mean CO_2 concentration [units: ppmv]. Thick red lines are from the simulated ensemble mean of the AllForc experiments by SPEAR, whereas thin red lines are from each member. Black lines in (a) and (b) are from observations (IBTrACS, *3*), whereas back line in (d) is from observations at Mt. Mauna Loa in Hawaii (online available at https://www.esrl.noaa.gov/gmd/ccgg/trends/data.html). This figure highlights that global TC number is projected to decrease toward the end of this century (Fig. S3a) due to substantial increases in greenhouse gases (Fig. S3d). However, the simulated TC number in the North Atlantic (Fig. S3b) moderately correlates with simulated anthropogenic aerosols during 1960–2020 in the way that simulated number of TCs shows lower around 1980 when sulfate aerosols over the North Atlantic show higher (Fig. S3c), whereas simulated TC number in the North Atlantic shows an increasing trend between 1980–2020 when simulated anthropogenic aerosols shows a decreasing trend over the period (Fig. S3c). Despite the projected low level of anthropogenic aerosols after 2020 (Fig. S3c), projected TC number in the North Atlantic continues to decrease (Fig. S3b), indicating that effect of greenhouse gases dominates in the future for the decreases in TC number in the North Atlantic.

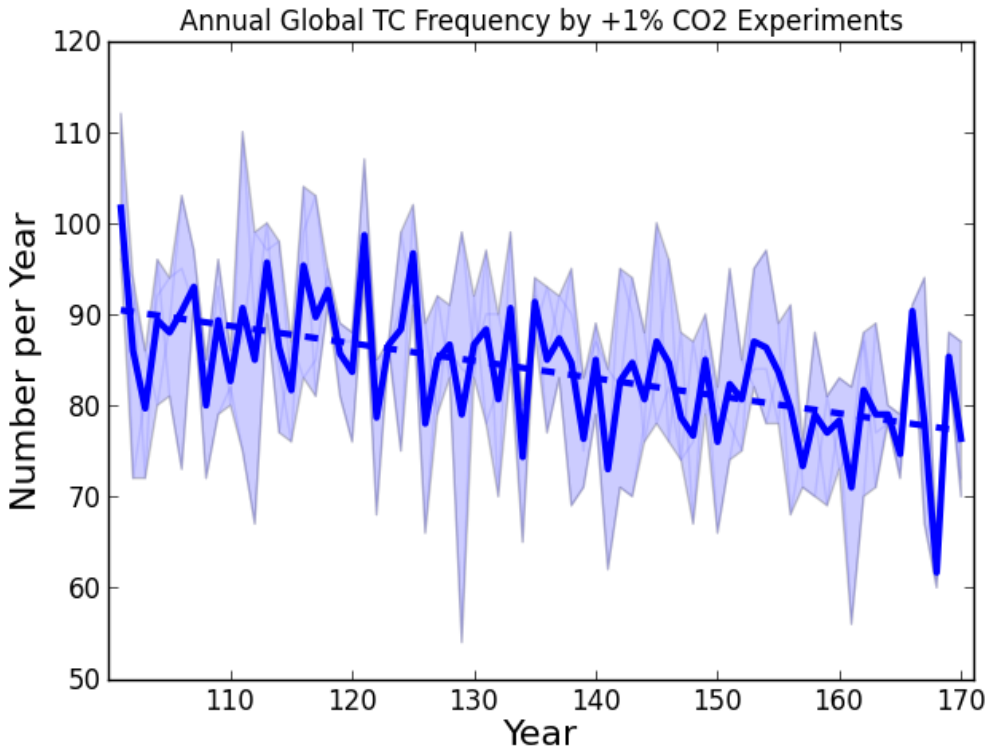

Fig. S4. Time series of simulated global TC number by Transient 2×CO_2 experiments.
Simulated global TC number [units: number per year] by 3-member Transient 2×CO2 experiments. Shadings indicates the minimum and maximum ranges among the ensemble members. Dashed line indicates a linear regression line. The negative linear trend is statistically significant at the 95% level according to the Mann–Kendall significance test. Between simulation year 101 to 170, CO_2 increases +1 % per year.

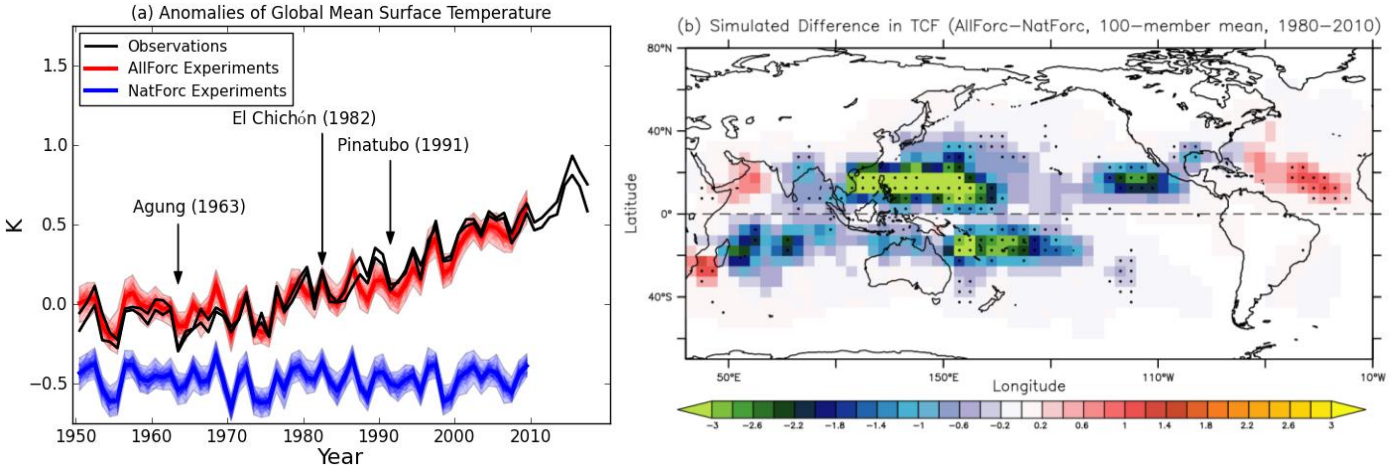

Fig. S5. Simulated anomalies of global mean surface temperature and TCF by the MRI large-ensemble simulations.

To reveal the robustness of the results with FLOR and SPEAR, we also analyzed the large-ensemble simulations of a different global climate model, MRI-AGCM (*4*–*5*). In the 100-member AllForc experiments, the observed time-varying monthly SSTs were prescribed along with the time-varying historical anthropogenic and natural forcing for the period 1951–2010. Differences among the ensemble members had small noise in the prescribed SSTs. The NatForc experiments were the same as AllForc, but with the detrended SSTs along with fixed anthropogenic forcing at the 1850 level assuming the pre-industrial conditions. Panel (a) shows the anomalies of global mean surface temperature relative to the mean of 1961–1990 simulated by AllForc (red) and NatForc (blue) along with observations (black). Note that, unlike AllForc and NatForc in FLOR and SPEAR, the observed interannual variation was retained in the prescribed SSTs among the ensemble members in both AllForc and NatForc with MRI-AGCM. Panel (b) reveals the difference in simulated TCF between AllForc and NatForc for the period 1980–2010. Because the interannual variation in SSTs was in phase among the all the ensemble members for AllForc and NatForc, the mean difference in TCF between the AllForc and NatForc represents a response of TCF to increases in anthropogenic forcing. The black dots in (b) indicate the difference in TCF is statistically significant at the 95% level according to a bootstrap method (*6*). Highlighted here, in Fig. S5b, is a similar spatial pattern to the trends of TCF simulated by FLOR and SPEAR (Fig. 1e), except for an inconsistent sign of change over the central Pacific.

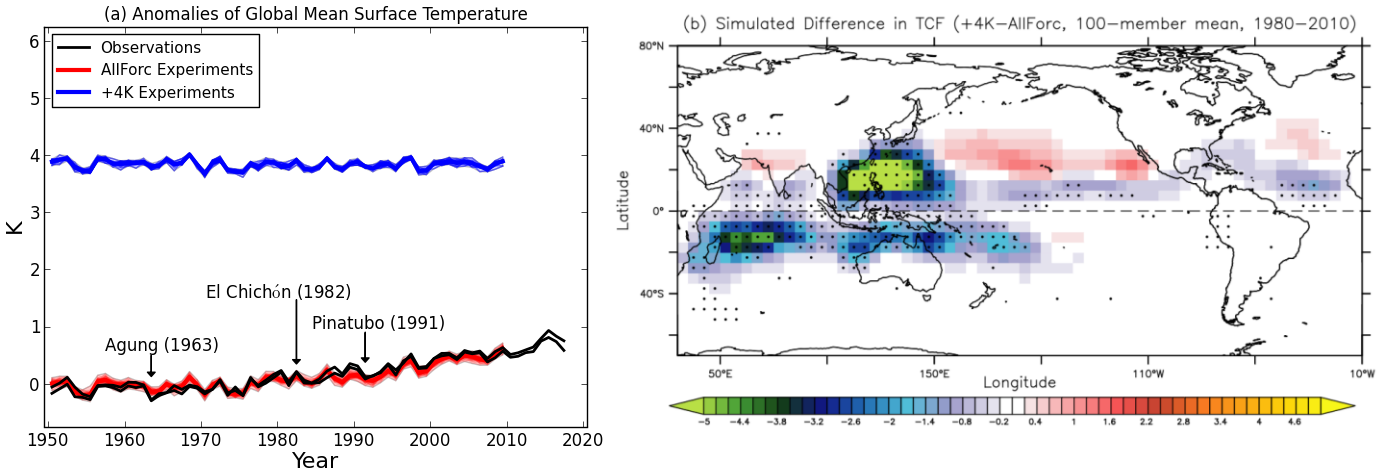

Fig. S6. As in Fig. S5, but with +4K experiments.

To reveal more clearly the potential impact of increases in anthropogenic forcing on global TCF changes, the 90-member ensemble experiments with strong anthropogenic forcing (e.g., +4K SST warming and quadrupled CO_2) were conducted and compared with the AllForc experiments using MRI-AGCM [see Mizuta et al. (*4*) and Yoshida et al. (*5*) for more details]. In the +4K experiments, the model was integrated for 60 years with the greenhouse-gas forcing set to the values at 2090 of the RCP8.5 scenario of CMIP5. Corresponding to the greenhouse-gas forcing, the global-mean surface temperature was set to be 4-K warmer than that of the present-day climate (Fig. 6Sa). The 4-K SST warming was not globally uniform, but had spatial patterns based on the RCP8.5 warming experiments in the CMIP5 models. The warming simulations explored the potential changes in the SST pattern by using six rescaled change patterns from CMIP5 models. Meanwhile, the observed interannual variation of SSTs was retained in the prescribed SSTs for the +4K experiments, as in the AllForc experiments (blue, red, and black lines in Fig. S6a). Panel (b) reveals the projected changes in TCF by the +4K experiments relative to the AllForc experiments using MRI-AGCM. Highlighted is a similar spatial pattern of TCF changes to that of the trends in the Transient CO_2 experiments with FLOR and SPEAR (Fig. 2n).

Table S1. Simulation configuration.

Three models (FLOR, FLOR-FA, and SPEAR) were used for the suite of simulations. The table shows the simulation names, models employed, periods used for analysis, the external forcing, number of ensemble members, whether or not there was volcanic forcing, and whether or not flux adjustment was applied.

Name	Model	Period	External Forcing	Ensemble Member	Volcanic Forcing	Flux Adjustment
piControl	FLOR-FA	Last 1,000 yrs of 3,500 yrs	Non-evolving emissions of gases, aerosols assuming pre-industrial conditions	1	No	Yes
	SPEAR	Last 1,000 yrs of 3,000 yrs				No
Transient $2\times CO_2$	FLOR	70 yrs	1% per year increase in CO_2 from 353 ppm to 707 ppm	1	No	No
	FLOR-FA					Yes
	SPEAR					No
AllForc	FLOR	1941–2004	Time-varying historical natural and anthropogenic forcing	30	Yes	No
		2005–2050	Anthropogenic forcing under the RCP8.5 scenario		No	
	FLOR-FA	1941–2004	Time-varying historical natural and anthropogenic forcing	35	Yes	Yes
		2005–2050	Anthropogenic forcing under the RCP4.5 scenario		No	
	SPEAR	1921–2014	Time-varying historical natural and anthropogenic forcing	30	Yes	No
		2015–2100	Anthropogenic forcing under the SSP5-85 scenario		No	
NatForc	FLOR	1941–2050	Radiative forcing fixed at 1941 level	30	Yes	No
	FLOR-FA					Yes
	SPEAR	1921–2100	Radiative forcing fixed at 1921 level			No

Reference

1. B.J. Henley, J. Gergis, D.J. Karoly, S.B. Power, J. Kennedy, & C.K. Folland. A Tripole Index for the Interdecadal Pacific Oscillation. *Climate Dynamics*, **45(11-12)**, 3077–3090, doi: 10.1007/s00382-015-2525-1. (2015).
2. N.A. Rayner, D. E. Parker, E. B. Horton, C. K. Folland, L. V. Alexander, & D. P. Rowell. Global analysis of sea surface temperature, sea ice, and night marine air temperature since the late nineteenth century. *J. Geophys. Res*., **108**, 4407, doi: 10.1029/2002JD002670. (2003).
3. K.R. Knapp, M. C. Kruk, D. H. Levinson, H. J. Diamond, & C. J. Neuman. The international best track archive for climate stewardship (IBTrACS): Unifying tropical cyclone best track data, *Bull. Amer. Meteor. Soc.*, **91**, 363–376, doi: 10.1175/2009BAMS2755.1. (2010).
4. R. Mizuta et al. Over 5,000 years of ensemble future climate simulations by 60-km global and 20-km regional atmospheric models. *Bull. Amer. Meteor. Soc.*, **98,** 1383–1398, doi: 10.1175/BAMS-D-16-0099.1. (2017).
5. K. Yoshida, M. Sugi, R. Mizuta, H. Murakami, & M. Ishii. Future changes in tropical cyclone activity in high-resolution large-ensemble simulations. *Geophys. Res. Lett.*, **44(19),** 9910–9917, doi: 10.1002/2017GL075058. (2017).
6. H. Murakami, B. Wang, T. Li, & A. Kitoh. Projected increase in tropical cyclones near Hawaii. *Nat. Clim. Change*, **3**, 749-754, doi: 10.1038/nclimate1890. (2013).